Biosensors and Bioelectronics 144 (2019) 111641

Contents lists available at ScienceDirect

Biosensors and Bioelectronics

journal homepage: www.elsevier.com/locate/bios

A signal-on electrochemical aptasensor for rapid detection of aflatoxin B1 based on competition with complementary DNA

Chao Wang[a,b], Yapiao Li[a,b], Qiang Zhao[a,b,*]

[a] State Key Laboratory of Environmental Chemistry and Ecotoxicology, Research Center for Eco-Environmental Sciences, Chinese Academy of Sciences, Beijing, 100085, China

[b] University of Chinese Academy of Sciences, Beijing, 100049, China

ARTICLE INFO

Keywords:
Aptamer
Aflatoxin B1
Competitive
Electrochemistry
Sensor
Electrode

ABSTRACT

Aflatoxin B1 (AFB1) is the most toxic mycotoxin, causing harmful effects on human and animal health, and the rapid and sensitive detection of AFB1 is highly demanded. We developed a simple electrochemical aptasensor achieving rapid detection of aflatoxin B1 (AFB1). A short anti-AFB1 aptamer having a methylene blue (MB) redox tag at the 3′-end was immobilized on the surface of a gold electrode. In the absence of AFB1, a complementary DNA (cDNA) strand hybridized with the MB-labeled aptamer, causing MB apart from the electrode surface and low current of MB. In the presence of AFB1, AFB1 competed with the cDNA in the binding to the MB-labeled aptamer, and the aptamer-AFB1 binding caused formation of a hairpin structure, making the MB close to the electrode surface and current of MB increase. Under optimized conditions, we achieved detection of AFB1 over dynamic concentration range of 2 nM–4 μM by using this signal-on electrochemical aptasensor. This method only required a simple 5-min incubation of sample solution prior to rapid electrochemical sensing, more rapid than other electrochemical aptasensors. The sensor could be well regenerated and reused. This sensor allowed to detect AFB1 spiked in 20-fold diluted beer and 50-fold diluted white wine, respectively. It shows potential for detection of AFB1 in wide applications.

1. Introduction

Aptasensors utilizing aptamers as biological recognition element combine advantages of aptamer (e.g., small size, good thermostability, low cost, ease of chemical synthesis and functional labeling) (Feng et al., 2014; Liu et al., 2009; Song et al., 2008; Yousefi et al., 2019). According to different signal transduction strategies, aptasensors have included optical sensors, electrochemical sensors, electrochemiluminescence sensors, micromechanical sensors, and etc (Feng et al., 2014; Liu et al., 2009; Song et al., 2008; Yousefi et al., 2019). Electrochemical sensors offer strengths of simplicity, easy miniaturization, high sensitivity, and economy (Kimmel et al., 2012; Labib et al., 2016; Zhu et al., 2015), and electrochemical aptasensors have gained extensive and broad attentions in bioassays and biosensors for a wide range of targets (Feng et al., 2014; Liu et al., 2009; Song et al., 2008; Ravalli et al., 2016; Razmi et al., 2018; Vasilescu and Marty, 2016; Yousefi et al., 2019).

Aflatoxin B1 (AFB1) is one major component of the aflatoxins compounds that are naturally produced by several species of Aspergillus (Kumar et al., 2017; Nesbitt et al., 1962). AFB1 causes adverse effects on health of humans and animals because of its mutagenicity, teratogenicity, and carcinogenicity, and it is the most toxic mycotoxin (Kumar et al., 2017; Liu and Wu, 2010; Sarma et al., 2017). AFB1 has been classified as a Group 1 carcinogen by the International Agency for Research on Cancer (Liu and Wu, 2010; Marin et al., 2013; Sarma et al., 2017). Agriculture products (e.g., corn, groundnut, wheat and feedstuff) and many other foods can be contaminated by AFB1, causing health risks and damages in economy (Kumar et al., 2017; Marin et al., 2013). Therefore, monitoring AFB1 is of great importance in food safety and environmental analysis, and especially the rapid and sensitive detection of AFB1 on site is highly demanded (Koppen et al., 2010, Shephard, 2009). Currently, chromatography techniques are often used for detection of AFB1, such as high performance liquid chromatography (HPLC) and liquid chromatography-tandem mass spectrometry (LC-MS) (Koppen et al., 2010, Shephard, 2009). However, they need sophisticated and expensive instruments and well-trained personnel (Koppen et al., 2010), which are not well suitable for rapid and on-site analysis. Immunoassays and immunosensors are also

* Corresponding author. State Key Laboratory of Environmental Chemistry and Ecotoxicology, Research Center for Eco-Environmental Sciences, Chinese Academy of Sciences, Beijing, 100085, China.
E-mail address: qiangzhao@rcees.ac.cn (Q. Zhao).

https://doi.org/10.1016/j.bios.2019.111641
Received 26 June 2019; Received in revised form 21 August 2019; Accepted 26 August 2019
Available online 29 August 2019
0956-5663/

frequently used for AFB1 detection, and they are simple and time-saving, but the antibodies have some shortcomings in preparation, cost and stability (Li et al., 2009; Peltomaa et al., 2018; Vidal et al., 2013).

Integrating the merits of anti-AFB1 aptamers and electrochemical sensing, electrochemical aptasensors for AFB1 have been developed, showing potential for on-site detection of AFB1 and overcoming the limitations of immunosensors and chromatography based methods (Abnous et al., 2017; Danesh et al., 2018; Geleta et al., 2018; Wu et al., 2017; Goud et al., 2016). Abnous et al. introduced an electrochemical sensing platform for detection of AFB1 using a π-shape structure consisting of aptamer and its complementary strands on the surface of electrode as a physical barrier (Abnous et al., 2017). Upon the addition of AFB1, the π-shape structure was disassembled and a strong current was recorded following the addition of exonuclease I. However, these reported electrochemical aptasensors usually need complex fabrication procedure, tedious reaction steps, and long-time sample incubation, and some of them need 1 h or a few hours in sample incubations (Abnous et al., 2017; Danesh et al., 2018; Wu et al., 2017; Goud et al., 2016; Geleta et al., 2018). In addition, some electrochemical aptasensors for AFB1 can not be reused. Therefore, these electrochemical aptasensors do not meet requirement for rapid detection of AFB1.

Here we reported a simple electrochemical aptasensor for rapid detection of AFB1. In our strategy, a short 28-mer anti-AFB1 thiolated aptamer sequence having a methylene blue (MB) label on the 3′-end was immobilized on a gold electrode. When AFB1 was absent in the sample solution, a complementary DNA strand (cDNA) of aptamer hybridized with the immobilized aptamer to form a rigid duplex DNA structure, making MB far from the electrode surface and generating low current. In the presence of AFB1, AFB1 competed with cDNA in the binding to MB-labeled aptamer. AFB1-aptamer binding caused formation of a hairpin structure and made MB close to electrode surface, so current increased. After optimizations of a series of experimental conditions, we achieved detection of AFB1 over a concentration range from 2 nM to 4 μM, with a detection limit of 2 nM. This sensing procedure was simple and rapid, and it only required 5-min incubation of sample solution before fast square wave voltammetry (SWV) analysis. This sensor could be reused due to good regeneration. This aptasensor is promising for AFB1 detection in applications.

2. Materials and methods

2.1. Materials and reagents

One short anti-AFB1 aptamer (5′-GCACGTGTTGTCTCTCTGTGTCT CGTGC-3′) was thiolated at the 5′-end and labeled with methylene blue (MB) at the 3′-end, named as MB-Apt (Le et al., 2012; Li et al., 2018). The MB-Apt and its partially complementary DNA (cDNA) strands were synthesized and purified by Sangon Biotech (Shanghai, China). The detailed sequences were listed in Table S1 in Electronic Supplementary Material (ESM). Aflatoxin B1 (AFB1), ochratoxin A (OTA), ochratoxin B (OTB), fumonisins B1 (FB1), fumonisins B2 (FB2), zearalenone (ZAE), other mycotoxins, and a PriboFast® Aflatoxin B_1 ELISA kit were obtained from Pribolab (Singapore). Tris-(2-carboxyrthyl) phosphine hydrochloride (TCEP) and 6-mercaptohexanol (MCH) were purchased from Sigma-Aldrich Co., Ltd. (St. Louis, USA). Beer and white grape wine were bought from a local supermarket. The following buffers were used. 1 × PBS buffer (pH 7.5) contained 137 mM NaCl, 2.7 mM KCl, 10 mM Na_2HPO_4 and 2 mM KH_2PO_4. Electrolyte buffer (E-buffer) for square wave voltammetry (SWV) measurements consisted of 1 × PBS (pH 7.5) and a certain concentration of $MgCl_2$. Aqueous solutions were prepared with ultrapure water (> 18.2 MΩ cm) from a Purelab Ultra Genetic Elga Labwater system (UK).

Electrochemical measurements were performed on an electrochemical workstation (CHI 660E, CH Instrument Co., Shanghai). All experiments were carried out with a conventional three-electrode system. The working electrode was a modified gold electrode (2 mm diameter). The counter electrode was a platinum wire, and the reference electrode was an Ag/AgCl (3 M KCl) electrode.

2.2. Preparation of the aptamer modified electrode

The DNA modified electrode was prepared by following the previously reported procedure (Xiao et al., 2007). The gold electrode (2 mm diameter) was first polished to a mirror-like surface by using 0.05 μm alumina slurries on a microcloth, followed by ultrasonic cleaning with water, ethanol, and water, respectively. After that, the electrode was electrochemically cleaned according to previous report (Xiao et al., 2007), and the details were shown in ESM.

Prior to immobilization, the thiolated aptamer (MB-Apt) was mixed with fresh TCEP (1 mM) in 1 × PBS (pH 7.5) solution, and incubated at 4 °C for 1 h. Then, we immersed the gold electrode in 50 μL of immobilization buffer (1 × PBS (pH 7.5) containing a certain concentration of activated MB-Apt for 1 h to obtain the MB-Apt modified gold electrode. Subsequently, the MB-Apt modified gold electrode was placed in 1 × PBS (pH 7.5) containing 2 mM MCH for 2 h to passivate the gold electrode surface. After washing, the MCH/MB-Apt modified gold electrode was finally obtained and ready for use.

2.3. AFB1 detection

The MCH/MB-Apt modified electrode was incubated in the sample solution containing AFB1 and cDNA in E-buffer (50 μL) for 5 min at 4 °C. Then, the electrode was washed with E-buffer, and square wave voltammetry (SWV) analysis was performed in 3 mL of E-buffer. The peak current of MB at about −0.25 V was measured. The following parameters were set, scanning range from 0 to −0.5 V, step potential of 1 mV, frequency of 60 Hz, and amplitude of 25 mV. Each measurement was repeated at least three times, and the height of current peak (ip) was recorded. After sensing, the electrode was regenerated by immersing the electrode in NaCl solution (5 M) for 10 min, followed by washing with deionized water for 3 min to remove the cDNA and the bound AFB1.

3. Results and discussions

3.1. Principle of electrochemical aptasensor for AFB1

Scheme 1 shows the principle of our electrochemical aptasensor for detection of AFB1. The anti-AFB1 aptamer having a methylene blue (MB) label at the 3′-end is immobilized on the surface of a gold electrode through the gold-sulfur chemistry. In the absence of AFB1, the cDNA hybridizes with the aptamer on the surface to form a rigid duplex DNA structure, making MB distant from the gold electrode surface and causing low peak current of MB due to the weak electron transfer efficiency between MB and electrode surface. In the presence of AFB1, competition between AFB1 and cDNA in the binding to the aptamer occurs, and when the aptamer binds with AFB1 instead of the cDNA, a hairpin structure is formed. Thus, the MB is close to the gold electrode surface, and the peak current of MB increases. Detection of AFB1 with signal-on response is achieved. A 28-mer DNA aptamer against AFB1 is used to fabricate the electrochemical aptasensor in our strategy, which is truncated from a long sequence of aptamer against AFB1 (Le et al., 2012; Li et al., 2018). This aptamer has a simple stem-loop secondary structure (Scheme 1) and shows high binding affinity to AFB1 (Le et al., 2012; Li et al., 2018; Sun and Zhao, 2018). The dissociation constant (K_d) of the aptamer against AFB1 is reported to be around tens nM level (Le et al., 2012; Sun et al., 2017; Sun and Zhao, 2018).

3.2. Characterization of the electrochemical aptasensor

To monitor the fabrication processes of the aptasensor, cyclic voltammetry (CV) and electrochemical impedance spectroscopy (EIS)

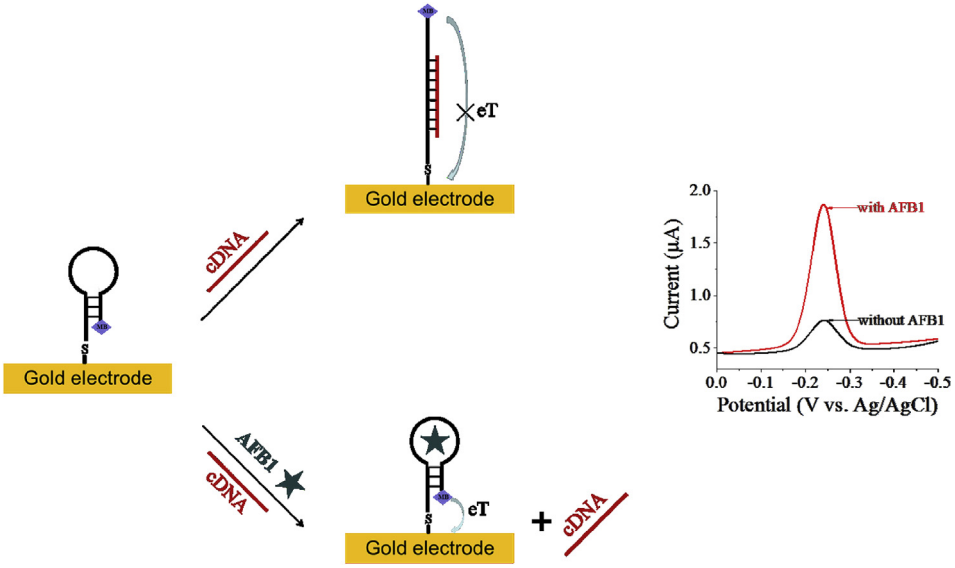

Scheme 1. Schematic diagram of the signal-on electrochemical aptasensor for AFB1 detection by using a gold electrode modified with aptamer having MB label at the terminal and a complementary DNA (cDNA). Detection of AFB1 is achieved by measuring the change of current of MB label.

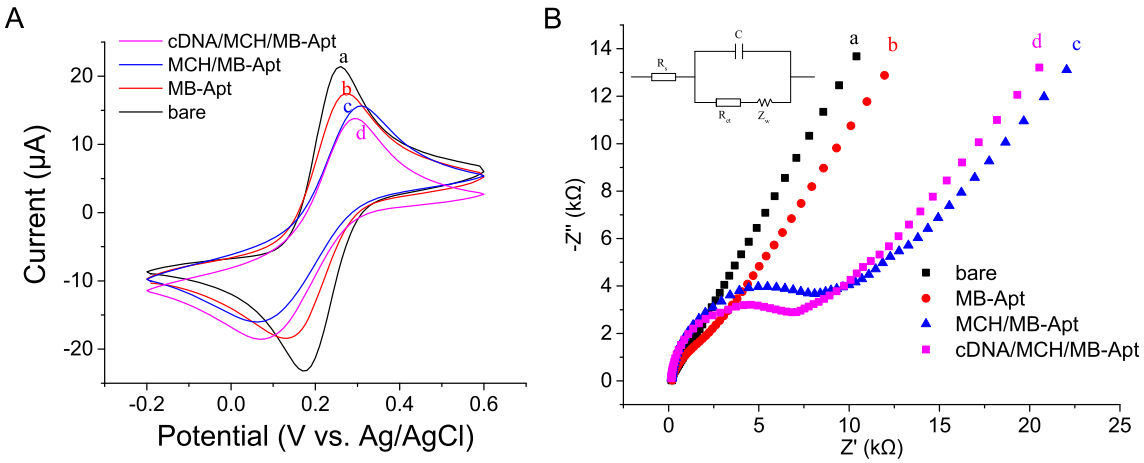

Fig. 1. (A) CV curves and (B) EIS spectra of (a) the bare gold electrode, (b) the MB-Apt modified gold electrode, (c) the MCH/MB-Apt modified gold electrode and (d) the cDNA/MCH/MB-Apt modified gold electrode. All measurements were carried out in a buffer solution, 10 mM Tris-HCl (pH 7.5) containing 0.1 M KCl and 5 mM $[Fe(CN)_6]^{4-/3-}$. CV was conducted in the potential range from −0.2 V to 0.6 V at a scan rate of 50 mV/s. In EIS experiment, frequency in the range of 0.1 Hz–10 kHz with amplitude of 250 mV was applied. Equivalent circuit corresponding to the EIS spectrum was shown. R_s and R_{et} were electrolyte and electron transfer resistances, Z_w was the Warburg impedance, and C was the capacitance of the electrode surface/solution interface. (For interpretation of the references to colour in this figure legend, the reader is referred to the Web version of this article.)

measurements were performed in each step. As Fig. 1A shows, a pair of well reversible redox peaks were observed on the bare gold electrode, which is ascribed to the high electron transfer efficiency between $[Fe(CN)_6]^{4-/3-}$ in solution and electrode surface. Immobilization of MB-Apt led to decrease of the peak currents, which is attributed to that the negatively charged MB-Apt bound on electrode surface repels $[Fe(CN)_6]^{4-/3-}$ anion (Table S2 in ESM). After blocking the electrode with MCH, the peak current further decreased, which may be due to the MCH layer formed on electrode surface hinders the diffusion of ferricyanide towards the electrode surface. After incubation of the MCH/MB-Apt modified electrode with cDNA, a slight increase in the redox peak current of ferricyanide was observed, which may be explained by hybridization makes the negatively charged MB-Apt strand upstanding, and the steric hindrance near electrode surface is decreased. In the EIS, the semicircle portion observed at high frequencies corresponds to the electron transfer limiting process (Castillo et al., 2015). The electron transfer resistance (R_{et}) values of the corresponding electrodes were calculated and summarized in Table S3 in ESM (Castillo et al., 2015). As shown in Fig. 1B, the MB-Apt modified electrode showed a larger semicircular diameter than that of the bare electrode, meaning an increase of R_{et} of the electrode. Formation of MCH layer on the electrode surface further increased R_{et}. After hybridization, the cDNA/MCH/MB-Apt electrode showed a smaller semicircular diameter than that of the MCH/MB-Apt electrode, indicating a decrease in R_{et}. This is due to the decrease of steric hindrance that is caused by hybridization between cDNA and MB-Apt immobilized on electrode. The R_{et} values corresponding different electrodes were shown in Table S3 in ESM. These results of EIS measurements are consistent with those of CV experiments. Both of CV and EIS analysis verified the electrochemical aptasensor was successfully fabricated.

3.3. Feasibility of the electrochemical aptasensor for AFB1 detection

To test the feasibility of the proposed electrochemical aptasensor for AFB1 detection, we incubated the MCH/MB-Apt modified gold electrode with cDNA in E-buffer solution in the absence of or in the

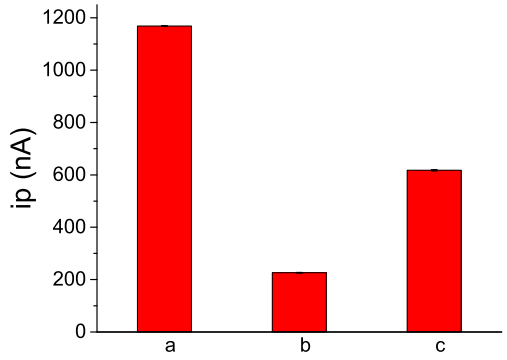

Fig. 2. Feasibility test of the electrochemical aptasensor. Peak currents of MB of the MCH/MB-Apt modified gold electrode (ip) were recorded. (a) before incubation of sample solution (corresponding to $ip_{initial}$); (b) after incubation with sample containing cDNA (corresponding to ip_{blank}); (c) after incubation with sample containing cDNA and AFB1 (200 nM) (corresponding to ip_{AFB1}). Experimental conditions: 100 nM MB-Apt in immobilization buffer, 200 nM cDNA (C14) in sample solution, E-buffer containing 20 mM $MgCl_2$, and incubation at 4 °C for 5 min.

presence of AFB1 (200 nM). After that, the electrode was washed with E-buffer, and SWV measurements of electrodes were conducted, and the peak current of MB at about −0.25 V was measured. As Fig. 2 shows, in comparison to the initial peak current ip value ($ip_{initial}$) without incubation of cDNA, the peak current value corresponding to the solution only containing cDNA (ip_{blank}) significantly decreased. This result suggests the hybridization between MB-Apt and cDNA drifted MB label apart from electrode surface, causing low electron transfer between MB and electrode surface. When AFB1 was present in the solution containing cDNA, the corresponding peak current (ip_{AFB1}) was much higher than ip_{blank}, demonstrating the competition between cDNA and AFB1 occurred in the binding with the aptamer on the electrode, and the aptamer bound with AFB1 instead of cDNA. Therefore, it is feasible to detect AFB1 by this electrochemical aptasensor with a signal-on response.

After detection of target, the electrochemical aptasensor was regenerated to remove the hybridized cDNA and the bound AFB1 by a simple incubation of NaCl solution (5 M) for 10 min and subsequent washing with ultrapure water for 3 min. At this condition, the binding affinity of the aptamer was significantly decreased (Sun et al., 2017; Sun and Zhao, 2018), and AFB1 was dissociated from the aptamer. The cDNA was also released from the aptamer because the hydrogen bonding became weak. Although there were some reductions of the $ip_{initial}$ (Fig. S1 in ESM) after cycles of regeneration processes, the electrochemical aptasensor still showed good response to AFB1. This result suggests this electrochemical aptasensor can be reused.

3.4. Optimization of experimental conditions

To achieve better analytical performance of this proposed aptasensor, some factors including length of cDNA, concentration ratio between cDNA and MB-Apt ($C_{cDNA}/C_{MB\text{-}Apt}$), amount of MB-Apt in immobilization buffer, incubation time, and incubation temperature were investigated.

The cDNA lengths had large effects on performance of this electrochemical aptasensor in detection of AFB1. As shown in Fig. 3A, ip_{blank} decreased with the increase of cDNA length, because longer cDNA facilitated the hybridization between cDNA and MB-Apt and more duplex of cDNA and aptamer was formed. When cDNA having more than 14 nucleotides was used, the obtained ip_{blank} was low and did not further decrease with the increase of length of cDNA. In all cases, the presence of AFB1 caused peak current higher than ip_{blank}. However, when cDNA was too long, the binding between aptamer and the cDNA was too strong, and it became difficult for AFB1 to compete

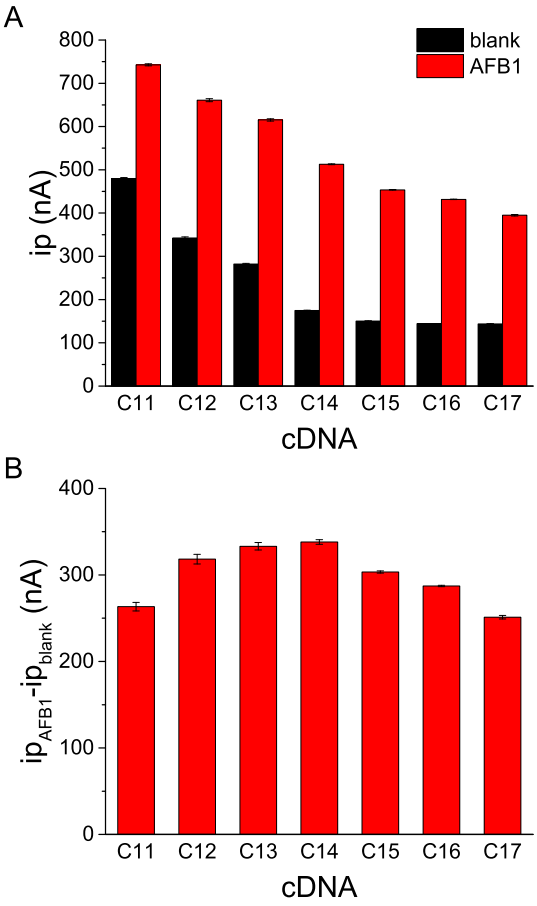

Fig. 3. (A) Peak current ip value of the MCH/MB-Apt electrode after incubation with different cDNAs in sample solution in the absence of or in the presence of 200 nM AFB1. (B) Effects of lengths of cDNA on signal change (ip_{AFB1}-ip_{blank}) caused by AFB1. 50 nM MB-Apt in immobilization buffer, 100 nM cDNA in sample solution, 20 mM $MgCl_2$ in E-buffer, and incubation at 4 °C for 5 min were applied. (For interpretation of the references to colour in this figure legend, the reader is referred to the Web version of this article.)

with the cDNA (Li et al., 2018), so the response of the aptasensor to AFB1 (200 nM) was reduced (Fig. 3B). The maximum current change caused by AFB1 (ip_{AFB1}-ip_{blank}) was obtained when C14 (cDNA containing 14 nucleotides) was used. Therefore, C14 was chosen as the preferable cDNA.

We further explored the influence of the ratio between concentration of cDNA in sample solution and concentration of MB-Apt in immobilization buffer ($C_{cDNA}/C_{MB\text{-}Apt}$) at 1:1, 2:1, 3:1 and 4:1, respectively. As shown in Fig. S2 in ESM, ip_{blank} value decreased with increasing value of $C_{cDNA}/C_{MB\text{-}Apt}$, which can be explained by increasing concentration of cDNA would enhance the hybridization with MB-Apt immobilized on electrode. The maximum current change caused by AFB1 (ip_{AFB1}-ip_{blank}) was obtained when $C_{cDNA}/C_{MB\text{-}Apt}$ was 2:1. Therefore, the $C_{cDNA}/C_{MB\text{-}Apt}$ was fixed at 2:1 in the further experiments.

The $MgCl_2$ concentration in E-buffer had great influence on the sensing performance of the aptasensor (Fig. S3 in ESM). With the increase of $MgCl_2$, the ip_{blank} decreased. This result can be attributed to that the presence of Mg^{2+} can enhance the hybridization of aptamer and its cDNA, causing the MB group apart from the gold electrode surface. The current change caused by AFB1 (ip_{AFB1}-ip_{blank}) increased and reached a plateau level at 20 mM $MgCl_2$. This result can be explained by that Mg^{2+} is helpful for the affinity binding between AFB1 and its aptamer (Li et al., 2018; Sun et al., 2017; Sun and Zhao, 2018). Based on these results, the E-buffer used in the experiments always

contained 20 mM $MgCl_2$.

The concentration of MB-Apt for electrode modification also had influence on this aptasensor. As shown in Fig. S4 in ESM, with the increasing MB-Apt concentration from 10 to 200 nM, the ip_{blank} values increased, suggesting the amount of MB-Apt on the electrode increased. When MB-Apt concentration was further increased from 200 to 500 nM, ip_{blank} values began to decrease. This result indicates that when too much MB-Apt was modified on the electrode, the MB-Apt on the electrode is crowded, and the MB was repelled distant from the electrode surface. The maximum signal change caused by AFB1 (ip_{AFB1}-ip_{blank}) was achieved when 100 nM MB-Apt was in the immobilization buffer. Therefore, immobilization buffer containing 100 nM MB-Apt was chosen for modification of MB-Apt on the electrode.

The time for incubating sample solution also had influence on the response of the aptasensor. As shown in Fig. S5 in ESM, ip_{blank} and ip_{AFB1} decreased with the increase of incubation time, and so did the ip_{AFB1}-ip_{blank} value, demonstrating the hybridization between MB-Apt and C14 was enhanced with increase of incubation time and longer incubation time was not favorable for AFB1 to compete with cDNA in the binding to the aptamer. 5 min incubation was optimal because the maximum current change caused by AFB1 (ip_{AFB1}-ip_{blank}) was obtained at this condition, and this condition is preferred for rapid analysis and higher sensitivity. The incubation at 4 °C was preferred for the electrochemical sensor to give better responses to AFB1, while the incubation at room temperature (25 °C) produced poor responses to target (Fig. S6 in ESM). The low temperature is helpful for AFB1 to compete with the cDNA in the binding to the immobilized aptamer.

3.5. Detection of AFB1

We successfully detected various concentrations of AFB1 by using this electrochemical aptasensor, under the optimum conditions (100 nM MB-Apt in immobilization buffer, 200 nM C14 in sample solution, 20 mM $MgCl_2$ in E-buffer, and incubation at 4 °C for 5 min). Fig. 4 shows SWV responses of the aptasensor to varying concentrations of AFB1. The current peak of MB at about −0.25 V increased with the increase of AFB1 concentration ranging from 2 nM to 4 μM. A good linear relationship between ip value and logarithmic concentration of AFB1 in the range of 8 nM to 4 μM was obtained (Fig. 4B). The correlated linear equation was y = 273.69lgx-25.38 (R^2 = 0.9918), where x was AFB1 concentration, and y was the ip value. The limit of detection (LOD) for AFB1 was determined to be 2 nM, based on signal change was three times of standard deviation of blank sample signal. The limit of quantitation for AFB1 was determined to be 8 nM, based on signal change was ten times of standard deviation of blank sample signal. Although the sensitivity is not higher than that of some previous reports (Abnous et al., 2017; Castillo et al., 2015; Evtugyn et al., 2014; Goud et al., 2017; Wu et al., 2017, 2019; Goud et al., 2016; Zheng et al., 2016) (Table S4 in ESM), our electrochemical aptasensor shows advantages of simple operation and rapid analysis. Only 50 μL of sample solution was needed for AFB1 detection in our work. In addition, this aptasensor can be reused with good regeneration by simple incubation with high concentration of NaCl solution. For the same modified electrode, the relative standard deviation (RSD) of signals for three different measurements after regeneration was less than 4%. For three independent modified electrode, the measurement of the same sample, the RSD was less than 6%. In addition, this electrochemical aptasensor still showed good response to AFB1 after storage of the MCH/MB-Apt modified gold electrode in the E-buffer at 4 °C for one week without losing activity. This result demonstrates the electrochemical aptasensor has good stability.

3.6. Specificity test

To test the specificity of this electrochemical aptasensor for AFB1, we analyzed AFB1 along with other mycotoxins including OTA, OTB, FB1, FB2, and ZAE. As shown in Fig. 5, only in the presence of AFB1 a large increase of ip value over the blank signal was observed, and this aptasensor did not show significant responses to other tested compounds. The coexistence of the tested other mycotoxins (OTA, OTB, FB1, FB2, and ZAE) and AFB1 did not cause interference to AFB1 detection. In addition, we tested other types of aflatoxins (AFB2, AFG1,

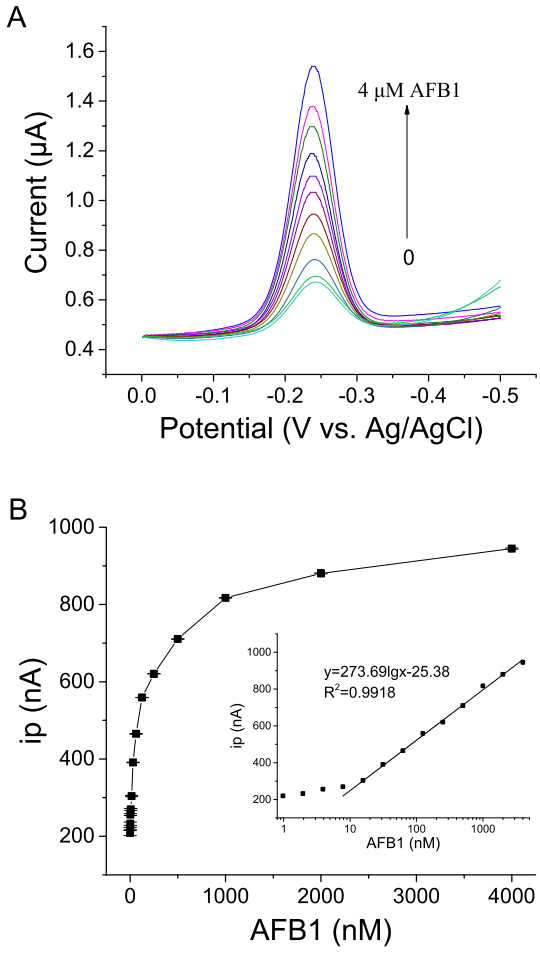

Fig. 4. (A) SWV responses of the electrochemical aptasensor to AFB1. (B) Relationship between peak currents of MB and the concentrations of AFB1. (For interpretation of the references to colour in this figure legend, the reader is referred to the Web version of this article.)

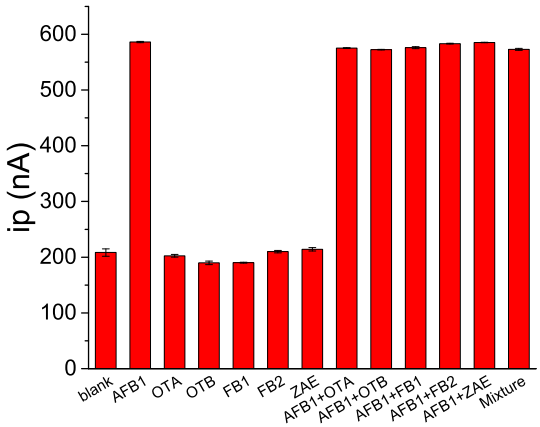

Fig. 5. Selectivity test of the electrochemical aptasensor for detection of AFB1. The tested non-target mycotoxins included OTA, OTB, FB1, FB2 and ZAE. The concentrations of AFB1 and non-target mycotoxins were 200 nM. The mixture contained all of the tested mycotoxins.

and AFG2), which have similar structures to AFB1 (Fig. S7 in ESM). The electrochemical sensor showed response to AFB2, AFG1, and AFG2, but the responses were lower than that from AFB1. It indicates AFB2, AFG1, and AFG2 can bind to the aptamer, and AFG1 and AFG2 show much weaker affinities to the aptamer, which is consistent with original report about the anti-AFB1 aptamer selection (Le et al., 2012). It is difficult for the aptamer to distinguish the difference between AFB1 and AFB2 because they have very similar structures. Our previous study also shows the cross-reactivities of the aptamer to AFB1, AFB2, AFG1, and AFG2 are about 100%, 61%, 6.3%, and 6.5% (Sun and Zhao, 2018). The presence of AFB2 can cause more interference than AFG1 and AFG2. A proper sample treatment or sample separation can be used to reduce the interference from other aflatoxins.

3.7. Detection of AFB1 in complex sample matrix

To evaluate the performance of the electrochemical aptasensor in complex sample matrixes, we tried to detect AFB1 spiked in 20-fold diluted beer or 50-fold diluted white grape wine by using this electrochemical aptasensor, respectively. The beer sample or white grape wine sample was diluted by the binding buffer solution. As displayed in Fig. S8, in both of the two complex sample matrixes, the electrochemical aptasensor responded well to the AFB1 over the range of 2 nM–4 μM. Linear relationships between ip value and logarithm of AFB1 concentration in the range of 8 nM to 4 μM were obtained. Correlated linear expressions are y = 274.14lgx-78.11 (R^2 = 0.9801) corresponding to 20-fold diluted beer samples, and y = 281.81lgx-48.87 (R^2 = 0.9932) corresponding to 50-fold diluted white grape wine samples, respectively (x is AFB1 concentration, and y is the ip value). The detection limits of AFB1 in the diluted beer and white wine were 2 nM. As comparison, we used a commercial ELISA kit and our electrochemical sensor to determine a certain concentration of AFB1 spiked in 20-fold diluted beer (Table S5 in ESM), and the determined AFB1 levels were close. This electrochemical aptasensor is promising in real-sample analysis.

4. Conclusion

In summary, we developed a simple signal-on electrochemical aptasensor allowing rapid detection of AFB1 based on the competition between AFB1 and the complementary DNA in the binding to the MB-labeled aptamer modified on gold electrode. This electrochemical aptasensor exhibited advantages of easy operation, rapid analysis, good regeneration and low cost. This electrochemical aptasensor enabled detection of AFB1 at 2 nM with 5-min sample incubation. It has potential for practical applications. As the aptamer itself can bind with other types of aflatoxins (AFB2, AFG1, and AFG2), a sample pretreatment will be needed to reduce the interference from other aflatoxins (especially the AFB2). Selection of more specific aptamer against AFB1 will also help. The sensitivity can be further improved by combining some signal amplification techniques.

CRediT authorship contribution statement

Chao Wang: Writing - original draft, Investigation. **Yapiao Li:** Investigation. **Qiang Zhao:** Conceptualization, Writing - review & editing, Funding acquisition.

Declaration of competing interest

The authors declare that they have no known competing financial interests or personal relationships that could have appeared to influence the work reported in this paper.

Acknowledgement

The financial support was from National Natural Science Foundation of China (Grant No. 21575153, 21435008, 21874146) and Strategic Priority Research Program of the Chinese Academy of Sciences (XDB14030200).

Appendix A. Supplementary data

Supplementary data to this article can be found online at https://doi.org/10.1016/j.bios.2019.111641.

References

Abnous, K., Danesh, N.M., Alibolandi, M., Ramezani, M., Emrani, A.S., Zolfaghari, R., Taghdisi, S.M., 2017. Biosens. Bioelectron. 94, 374–379.
Castillo, G., Spinella, K., Poturnayová, A., Šnejdárková, M., Mosiello, L., Hianik, T., 2015. Food Control 52, 9–18.
Danesh, N.M., Bostan, H.B., Abnous, K., Ramezani, M., Youssefi, K., Taghdisi, S.M., Karimi, G., 2018. Trac. Trends Anal. Chem. 99, 117–128.
Evtugyn, G., Porfireva, A., Stepanova, V., Sitdikov, R., Stoikov, I., Nikolelis, D., Hianik, T., 2014. Electroanalysis 26, 2100–2109.
Feng, C., Dai, S., Wang, L., 2014. Biosens. Bioelectron. 59, 64–74.
Geleta, G.S., Zhao, Z., Wang, Z., 2018. Analyst 143, 1644–1649.
Goud, K.Y., Hayat, A., Catanante, G., Satyanarayana, M., Gobi, K.V., Marty, J.L., 2017. Electrochim. Acta 244, 96–103.
Kimmel, D.W., LeBlanc, G., Meschievitz, M.E., Cliffel, D.E., 2012. Anal. Chem. 84, 685–707.
Koppen, R., Koch, M., Siegel, D., Merkel, S., Maul, R., Nehls, I., 2010. Appl. Microbiol. Biotechnol. 86, 1595–1612.
Kumar, P., Mahato, D.K., Kamle, M., Mohanta, T.K., Kang, S.G., 2017. Front. Microbiol. 7, 2170.
Labib, M., Sargent, E.H., Kelley, S.O., 2016. Chem. Rev. 116, 9001–9090 2016.
Le, L.C., Cruz-Aguado, J.A., Penner, G.A., 2012. USA Patent PCT/CA2010/001292.
Li, P., Zhang, Q., Zhang, W., 2009. Trac. Trends Anal. Chem. 28, 1115–1126.
Li, Y.P., Sun, L.L., Zhao, Q., 2018. Anal. Bioanal. Chem. 410, 6269–6277.
Liu, J., Cao, Z., Lu, Y., 2009. Chem. Rev. 109, 1948–1998.
Liu, Y., Wu, F., 2010. Environ. Health Perspect. 118, 818–824.
Marin, S., Ramos, A.J., Cano-Sancho, G., Sanchis, V., 2013. Food Chem. Toxicol. 60, 218–237.
Nesbitt, B.F., O'kelly, J., Sargeant, K., Sheridan, A., 1962. Nature 195, 1062–1063.
Peltomaa, R., Benito-Pena, E., Moreno-Bondi, M.C., 2018. Anal. Bioanal. Chem. 410, 747–771.
Ravalli, A., Voccia, D., Palchetti, I., Marrazza, G., 2016. Biosensors 6, 39.
Razmi, N., Baradaran, B., Hejazi, M., Hasanzadeh, M., Mosafer, J., Mokhtarzadeh, A., de la Guardia, M., 2018. Biosens. Bioelectron. 58–71.
Sarma, U.P., Bhetaria, P.J., Devi, P., Varma, A., 2017. Indian J. Clin. Biochem. 32, 124–133.
Shephard, G.S., 2009. Anal. Bioanal. Chem. 395, 1215–1224.
Song, S.P., Wang, L.H., Li, J., Zhao, J.L., Fan, C.H., 2008. Trac. Trends Anal. Chem. 27, 108–117.
Sun, L., Wu, L., Zhao, Q., 2017. Microchim.Acta 184, 2605–2610.
Sun, L., Zhao, Q., 2018. Talanta 189, 442–450.
Vasilescu, A., Marty, J.L., 2016. Trac. Trends Anal. Chem. 79, 60–70.
Vidal, J.C., Bonel, L., Ezquerra, A., Hernandez, S., Bertolin, J.R., Cubel, C., Castillo, J.R., 2013. Biosens. Bioelectron. 49, 146–158.
Wu, L., Ding, F., Yin, W., Ma, J., Wang, B., Nie, A., Han, H., 2017. Anal. Chem. 89, 7578–7585.
Wu, S.S., Wei, M., Wei, W., Liu, Y., Liu, S., 2019. Biosens. Bioelectron. 129, 58–63.
Xiao, Y., Lai, R.Y., Plaxco, K.W., 2007. Nat. Protoc. 2, 2875–2880.
Yousefi, M., Dehghani, S., Nosrati, R., Zare, H., Evazalipour, M., Mosafer, J., Tehrani, B.S., Pasdar, A., Mokhtarzadeh, A., Ramezani, M., 2019. Biosens. Bioelectron. 130, 1–19.
Goud, K.Y., Catanante, G., Hayat, A., Gobi, K.V., Marty, J.L., 2016. Sens. Actuators B Chem. 235, 466–473.
Zheng, W., Teng, J., Cheng, L., Ye, Y., Pan, D., Wu, J., Xue, F., Liu, G., Chen, W., 2016. Biosens. Bioelectron. 80, 574–581.
Zhu, C., Yang, G., Li, H., Du, D., Lin, Y., 2015. Anal. Chem. 87, 230–249.